Int. J. Heat Mass Transfer. Vol. 30, No. 4, pp. 623–630, 1987
Printed in Great Britain

0017–9310/87 $3.00+0.00

Conjugate natural convection about a vertical cylindrical fin with lateral mass flux in a saturated porous medium

JIN-YUAN LIU and SHAGI-DI SHIH
Department of Mathematics, University of Wyoming, Laramie, WY 82071, U.S.A.

and

W. J. MINKOWYCZ
Department of Mechanical Engineering, University of Illinois at Chicago, Chicago, IL 60680, U.S.A.

(*Received* 3 *July* 1986 *and in final form* 12 *September* 1986)

Abstract—The problem of conjugate natural convection about a vertical cylindrical fin with uniform lateral mass flux in a fluid-saturated porous medium has been studied numerically. Solutions based on the third level of truncation are obtained by the local nonsimilarity method. The effects of the surface mass flux, the conjugate convection–conduction parameter, and the surface curvature on fin temperature distribution, local heat transfer coefficient, local heat flux, average heat transfer coefficient, and total heat transfer rate are presented. A comparison with finite-difference solutions for the case of constant wall temperature was made, and found in a good agreement.

INTRODUCTION

THE ANALYSIS of conjugate heat transfer about a vertical fin has attracted considerable interest during the past few years. The basic feature which differs from the conventional fin theory or boundary layer flow analysis is that the heat transfer coefficient or thermal boundary conditions, instead of being prescribed as in conventional studies, are part of the solutions to the problem. This consideration is necessary and more realistic in many practical applications, particularly in the heat transfer analysis of extended surfaces, where the thermal boundary conditions are prescribed only at the ends of the surfaces. The close interactions between the conduction in the solid boundary and the convection in the adjacent boundary layer flow exhibit quite an unusual local behavior in heat transfer characteristics.

Conjugate heat transfer problems induced by various convection mechanisms (forced, free, mixed convection) about a flat plate or a cylindrical surface in Newtonian fluids have been investigated extensively [1–5]. Recently, Liu *et al.* [6, 7] have extended the analysis to include the conjugate mixed convection in porous media. However, in the above studies the influence of injection or withdrawal of fluids on conjugate heat transfer has not been attempted. In this paper we direct our attention to conjugate natural convection about a vertical cylindrical fin in porous media and to the effects of surface mass flux on heat transfer characteristics. Natural convection about a vertical cylinder in a porous medium has been discussed by Minkowycz and Cheng [8] for the case of power-law variations of the surface temperature, and the influence of uniform lateral mass flux on natural convection about a vertical cylinder with prescribed constant wall temperature or constant wall heat flux was analyzed by Yücel [9]. The present analysis is an extension of the previous work to include the conjugate effects on the heat transfer analysis.

Numerical solutions of the governing differential equations are generated by the local nonsimilarity method. Results are presented in tabular or graphic forms as functions of three dominant parameters: the transverse curvature parameter λ, the surface mass transfer parameter ω, and the conjugate convection–conduction parameter N_{cc}. A comparison was made with Yücel's results [9], which were obtained by finite difference method, for the case of constant wall temperature, and found in good agreement.

ANALYSIS

Consider a vertical cylindrical fin with length L and radius r_0 whose upper end is attached to a surface with temperature T_b. The fin with uniform blowing or suction rate v_w is situated in a quiescent fluid-saturated porous medium of temperature T_∞, which is assumed to be smaller than T_b. The coordinate system with the origin at the tip of the fin is oriented so that the positive x-axis is in the opposite direction to the gravitational acceleration and the r-axis is perpendicular to the fin surface.

If the radius of the fin r_0 is relatively small compared with its length, heat conduction in the fin can be

NOMENCLATURE

- f dimensionless stream function defined by equation (13)
- G auxiliary velocity function, $\partial f/\partial\xi$
- g acceleration due to gravity
- h local heat transfer coefficient
- h^* dimensionless local heat transfer coefficient
- H auxiliary velocity function, $\partial G/\partial\xi$
- K permeability of the porous medium
- k thermal conductivity of the porous medium
- k_f conductivity of the fin
- N_{cc} convection–conduction parameter, $(2kL/k_f r_0)\sqrt{Ra}$
- q local heat flux
- r coordinate in the transverse direction
- r_0 radius of the cylindrical fin
- Ra Rayleigh number, $g\beta K(T_b - T_\infty)L/\nu\alpha$
- T temperature
- u Darcy's velocity in the x-direction
- v Darcy's velocity in the r-direction
- x coordinate in the streamwise direction.

Greek symbols

- α equivalent thermal diffusivity
- β coefficient of thermal expansion
- η pseudosimilarity variable defined by equation (12)
- ξ dimensionless variable in the x-direction
- θ dimensionless temperature of the fluid defined by equation (14)
- θ_f dimensionless temperature for the fin defined by equation (15)
- λ transverse surface curvature parameter, $4L/r_0\sqrt{Ra}$
- μ viscosity of the convective fluid in the porous medium
- ν kinematic viscosity of the convective fluid
- ρ density of the convective fluid
- ϕ auxiliary temperature function, $\partial\theta/\partial\xi$
- χ auxiliary temperature function, $\partial\phi/\partial\xi$
- ψ stream function defined by equation (6)
- ω lateral mass transfer parameter, $v_\omega\sqrt{(\nu L/\alpha g\beta k(T_0 - T_\infty))}$.

Subscripts

- ∞ condition at infinity
- b condition at the fin base
- f variable associated with the fin.

approximated as one-dimensional. Accordingly, the equation governing the heat conduction is

$$\frac{d^2T_f}{dx^2} = \frac{2h(x)}{k_f r_0}(T_f - T_\infty) \tag{1}$$

where T_f is the temperature of the fin; $h(x)$ is the local heat transfer coefficient, which is unknown at present; k_f is the thermal conductivity of the fin. The boundary conditions for the fin are

$$x = L: \quad T_f = T_b \tag{2}$$

$$x = 0: \quad \frac{dT_f}{dx} = 0. \tag{3}$$

Here we have assumed that the heat loss from the tip of the fin is negligible.

A two-dimensional steady incompressible free convection boundary layer flow is considered here. With the Boussinesq approximations and Darcy's law being applicable, the governing equations in cylindrical coordinates for flow in the porous medium are [10]

$$\frac{\partial}{\partial r}\left(\frac{1}{r}\frac{\partial\psi}{\partial r}\right) = \frac{\rho_\infty g K\beta}{\mu}\frac{\partial T}{\partial r} \tag{4}$$

$$\frac{\partial}{\partial r}\left(r\frac{\partial T}{\partial r}\right) = \frac{1}{\alpha}\left(\frac{\partial\psi}{\partial r}\frac{\partial T}{\partial x} - \frac{\partial\psi}{\partial x}\frac{\partial T}{\partial r}\right). \tag{5}$$

The stream function ψ is defined as

$$u = \frac{1}{r}\frac{\partial\psi}{\partial r} \quad \text{and} \quad v = -\frac{1}{r}\frac{\partial\psi}{\partial r} \tag{6a, b}$$

where u and v are the Darcian velocities in the x- and r-directions. In the above equations, ρ_∞, μ and β are the density of the fluid at infinity, the viscosity, and the thermal expansion coefficient of the fluid, respectively; K and α are the permeability and equivalent thermal diffusivity of the porous medium; g is the gravitational acceleration, and T is the temperature of the porous medium.

Equations (4) and (5) are subject to the boundary conditions

$$r = r_0: \quad -\frac{1}{r}\frac{\partial\psi}{\partial x} = v_\omega, \quad T = T(x, r_0) \tag{7a, b}$$

$$r \to \infty: \quad \frac{\partial\psi}{\partial r} = 0, \quad T = T_\infty \tag{8a, b}$$

where v_ω is the surface mass transfer rate. It is positive for injection and negative for withdrawal; $T(x, r_0)$ is the temperature at the fin surface.

It should be noted that $h(x)$ and $T(x, r_0)$ are

unknowns in the above formulation. The conditions to be used to determine these quantities are

$$r = r_0: \qquad T(x, r_0) = T_f(x) \tag{9}$$

and

$$r = r_0: \qquad -k\frac{\partial T}{\partial r} = h(x)(T_f - T_\infty). \tag{10}$$

These two conditions state the physical requirements that at the solid–fluid boundary the temperatures and heat fluxes of the fin and the porous medium are continuous. Equations (1)–(10) constitute the mathematical modeling of the present analysis.

To facilitate our analysis, the above equations are nondimensionalized according to the following transformation:

$$\xi = \frac{x}{L} \tag{11}$$

$$\eta = \frac{r^2 - r_0^2}{4r_0}\sqrt{\left(\frac{\beta g K(T_b - T_\infty)}{x\nu\alpha}\right)} \tag{12}$$

$$\psi = r_0\sqrt{\left(\frac{\alpha g\beta K(T_b - T_\infty)x}{\nu}\right)} f(\xi, \eta) \tag{13}$$

$$\theta = \frac{T - T_\infty}{T_b - T_\infty} \tag{14}$$

$$\theta_f = \frac{T_f - T_\infty}{T_b - T_\infty}. \tag{15}$$

With this transformation, equations (1)–(5) and (7)–(10) become:

heat conduction for fin

$$\frac{d^2\theta_f}{d\xi^2} = (N_{cc})h^*(\xi)\theta_f \tag{16}$$

$$\xi = 0: \qquad \frac{d\theta_f}{d\xi} = 0 \tag{17}$$

$$\zeta = 1: \qquad \theta_f = 1 \tag{18}$$

boundary layer flow

$$\frac{\partial^2 f}{\partial\eta^2} = 2\frac{\partial\theta}{\partial\eta} \tag{19}$$

$$(1 + \lambda\sqrt{\xi}\eta)\frac{\partial^2\theta}{\partial\eta^2} + (f + \lambda\sqrt{\xi})\frac{\partial\theta}{\partial\eta} = 2\xi\left(\frac{\partial f}{\partial\eta}\frac{\partial\theta}{\partial\xi} - \frac{\partial\theta}{\partial\eta}\frac{\partial f}{\partial\xi}\right) \tag{20}$$

$$f(\xi, 0) = -2\left(\xi\frac{\partial f}{\partial\xi} + \omega\sqrt{\xi}\right), \quad \theta(\xi, 0) = \theta_f(\xi) \tag{21a, b}$$

$$f'(\xi, \infty) = 0, \qquad \theta(\xi, \infty) = 0 \tag{22a, b}$$

conditions at the solid–fluid interface

$$\eta = 0: \qquad \theta(\xi, 0) = \theta_f(\xi) \tag{23}$$

$$\eta = 0: \qquad h^*(\xi) = -\frac{1}{2}\frac{\left.\dfrac{\partial\theta}{\partial\eta}\right|_{\eta=0}}{\sqrt{\xi}\theta_f(\xi)} \tag{24}$$

where $N_{cc} = (2kL/k_f r_0)\sqrt{Ra}$ and $h^*(\xi) = hL/k\sqrt{Ra}$ are the conjugate convection–conduction parameter and dimensionless local heat transfer coefficient, respectively

$$Ra = \frac{g\beta K(T_b - T_\infty)L}{\nu\alpha}$$

is the modified Rayleigh number, $\lambda = 4L/r_0\sqrt{Ra}$ and

$$\omega = v_\omega\sqrt{\left(\frac{\nu L}{\alpha g\beta K(T_b - T_\infty)}\right)}$$

are transverse surface curvature parameter and lateral mass transfer parameter. ω is positive for injection and negative for withdrawal. It should be noted that N_{cc} is a ratio of convective effect to fin conductance. For the case $N_{cc} = 0$, it represents the free convection about an isothermal fin. Also one should note that λ is a measure of transverse curvature and for $\lambda = 0$, the geometry reduces to flat plate.

NUMERICAL SOLUTIONS

Equation (16) is coupled with equations (19) and (20) through the interfacial conditions, equations (23) and (24). The complete sets of equations, equations (16)–(22), must be solved simultaneously. Analytic solution does not seem feasible due to the nonlinearity of equation (20) as well as coupling of the system, and therefore the solution must be obtained numerically. The overall iterative solution procedure used was described in detail in refs. [6, 7].

It is seen that the boundary layer equations do not admit similarity solution due to the appearance of the surface curvature and nonisothermal boundary conditions. The numerical scheme adopted here to solve the boundary layer flow is the local nonsimilarity method described in refs. [10, 11]. Following the standard procedure, one can derive an approximate set of differential equations for each 'level of truncation'. The resulting differential equations and boundary conditions are presented below.

First level of truncation

$$f'' = 2\theta' \tag{25}$$

$$(1 + \lambda\sqrt{\xi}\eta)\theta'' + (f + \lambda\sqrt{\xi})\theta' = 0 \tag{26}$$

with

$$f(\xi, 0) = -2\omega\sqrt{\xi} \tag{27}$$

$$\theta(\xi, 0) = \theta_f(\xi) \tag{28}$$

$$f'(\xi,\infty)=0 \tag{29}$$

$$\theta(\xi,\infty)=0. \tag{30}$$

Second level of truncation

$$f''=2\theta' \tag{31}$$

$$(1+\lambda\sqrt{\xi\eta})\theta''+(f+\lambda\sqrt{\xi}+2\xi G)\theta'=2\xi f'\phi \tag{32}$$

$$G''=2\phi' \tag{33}$$

$$(1+\lambda\sqrt{\xi\eta})\phi''+(f+\lambda\xi+2\xi G)\phi'=2(f'+\xi G')\phi-\frac{\lambda\eta}{2\sqrt{\xi}}\theta''-\left(3G+\frac{\lambda}{2\sqrt{\xi}}\right)\theta' \tag{34}$$

with

$$f(\xi,0)=-\frac{4}{3}\omega\sqrt{\xi},\qquad G(\xi,0)=-\frac{1}{3}\frac{\omega}{\sqrt{\xi}} \tag{35a, b}$$

$$\theta(\xi,0)=\theta_f(\xi),\qquad \phi(\xi,0)=\frac{d\theta_f}{d\xi}(\xi) \tag{36a, b}$$

$$f'(\xi,\infty)=0,\qquad G'(\xi,\infty)=0 \tag{37a, b}$$

$$\theta(\xi,\infty)=0,\qquad \phi(\xi,\infty)=0. \tag{38a, b}$$

Third level of truncation

$$f''=2\theta' \tag{39}$$

$$(1+\sqrt{\xi\eta})\theta''+(\tfrac{1}{2}f+\lambda\sqrt{\xi}+2\xi G)\theta'=2\xi f'\phi \tag{40}$$

$$G''=2\phi' \tag{41}$$

$$(1+\lambda\sqrt{\xi\eta})\phi''+(f+\lambda\sqrt{\xi}+2\xi G)\phi=2(f'+\xi G')\phi+2\xi f'\chi-\frac{\lambda\eta}{2\sqrt{\xi}}\theta''-\left(3G+\frac{\lambda}{2\sqrt{\xi}}+2\xi H\right)\theta' \tag{42}$$

$$H''=2\chi' \tag{43}$$

$$(1+\lambda\sqrt{\xi\eta})\chi''+(f+\lambda\sqrt{\xi}+2\xi G)\chi'=4(f'+\xi G')\chi-\frac{\lambda\eta}{\sqrt{\xi}}\phi''-\left(6G+\frac{\lambda}{\sqrt{\xi}}+4\xi H\right)\phi'+2(2G'+\xi H')\phi+\frac{\lambda\eta}{4\xi\sqrt{\xi}}\theta''-\left(5H-\frac{\lambda}{4\xi\sqrt{\xi}}\right)\theta' \tag{44}$$

with

$$f(\xi,0)=-\frac{6}{5}\omega\sqrt{\xi},\qquad G(\xi,0)=-\frac{2}{5}\frac{\omega}{\sqrt{\xi}},\qquad H(\xi,0)=\frac{1}{10}\frac{\omega}{\sqrt{\xi^3}} \tag{45a–c}$$

$$\theta(\xi,0)=\theta_f(\xi),\qquad \phi(\xi,0)=\frac{d\theta_f}{d\xi}(\xi),\qquad \chi(\xi,0)=\frac{d^2\theta_f}{d\xi^2} \tag{46a–c}$$

$$f'(\xi,\infty)=0,\qquad G'(\xi,\infty)=0,\qquad H'(\xi,\infty)=0 \tag{47a–c}$$

$$\theta(\xi,\infty)=0,\qquad \phi(\xi,\infty)=0,\qquad \chi(\xi,\infty)=0. \tag{48a–c}$$

In the above equations, the primes are the derivatives with respect to η. The variables G, H, ϕ, and χ are defined as $G=\partial f/\partial\xi$, $H=\partial G/\partial\xi$, $\phi=\partial\theta/\partial\xi$, and $\chi=\partial\phi/\partial\xi$. It is pertinent to note that ξ plays the role of a parameter in the above equations.

Solutions of the above sets of ordinary differential equations may be obtained by various methods. Among others, one may recast the differential equations into integral forms and solve them by iteration. The details of this procedure were described in ref. [10]. To accommodate the fast variations of heat-transfer-related quantities in the regions near the tip of the fin and the solid boundary, a non-uniform mesh with smallest step size in these regions was chosen. A search for the value of η at infinity for each streamwise location was made to ensure that the value of f'' at infinity is less than 10^{-3}. This results in, for the selected values of λ, ω, and N_{cc}, a total of 33 points along the ξ-coordinate, and a minimum of 121 points near the fin tip and a maximum of 251 points near the fin base along the η-coordinate. The following results are based on the third level of truncation.

RESULTS AND DISCUSSION

It was noted that the present analysis includes the case of free convection about a vertical cylinder with constant temperature distribution. This corresponds to the case of $N_{cc}=0$. Solutions to this problem have also been obtained by Yücel [9], who has used the finite-difference method. Table 1 presents the values of $-\theta'(1,0)$ at the base of the fin ($\xi=1$) for various values of λ and ω both from the present analysis and from ref. [9]. It is seen that the results are in good agreement.

Results of fin temperature distribution, which serves as the thermal boundary conditions of the boundary layer flow, are presented in Figs. 1 and 2 for $\lambda=1$ and 3, respectively, for selected values of ω and N_{cc}. One sees that in all cases the fin temperature distribution increases monotonically from the tip of the fin ($\xi=0$) to the base. It is also seen that larger

Table 1. A comparison of values of $-\theta'(1,0)$ with those obtained by Yücel [9] for constant wall temperature

	(λ, ω)	Present analysis	Ref. [9]
No mass flux	(0.50, 0.0)	0.4888	0.4902
	(1.00, 0.0)	0.5321	0.5347
	(2.00, 0.0)	0.6145	0.6192
	(3.00, 0.0)	0.6945	0.6991
	(4.00, 0.0)	0.7721	0.7753
Withdrawal	(0.25, −0.0625)	0.4953	0.4957
	(0.50, −0.1250)	0.5475	0.5483
	(1.00, −0.2500)	0.6525	0.6543
	(1.50, −0.3750)	0.7610	0.7629
	(2.00, −0.5000)	0.8700	0.8722
Injection	(0.20, 0.075)	0.4283	0.4300
	(0.40, 0.150)	0.4152	0.4176
	(0.80, 0.300)	0.3925	0.3961
	(1.20, 0.450)	0.3745	0.3779
	(1.60, 0.600)	0.3604	0.3621
Plate fin	(0.0, 0.125)	0.3891	0.3904
	(0.0, 0.250)	0.3420	0.3422
	(0.0, 0.500)	0.2546	0.2595
	(0.0, 0.750)	0.1910	0.1934
	(0.0, 1.000)	0.1398	0.1415

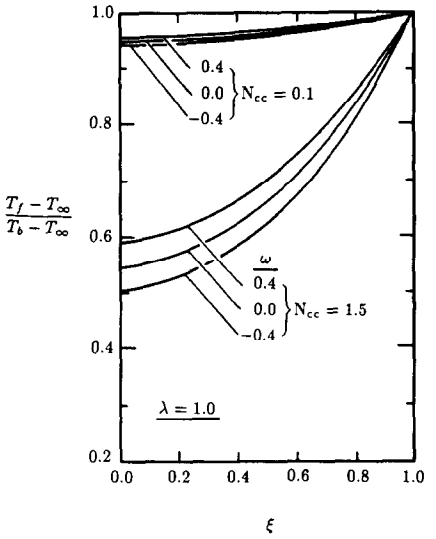

FIG. 1. Fin temperature distribution for $\lambda = 1.0$.

values of N_{cc} give rise to larger fin temperature variations. This behavior is evident from the definition of N_{cc}, which shows that higher values of N_{cc} correspond to low fin conductances and high convection effects, thus resulting in increased temperature variations. In addition, these figures show that withdrawal of fluid ($\omega < 0$) amplifies these variations while injection of fluid ($\omega > 0$) reduces variations. It will be seen later that this is due to the fact that withdrawal of fluid enhances the heat transfer rate, and accordingly increases the variations. The figures also demonstrate that higher values of λ give rise to larger fin temperature variations.

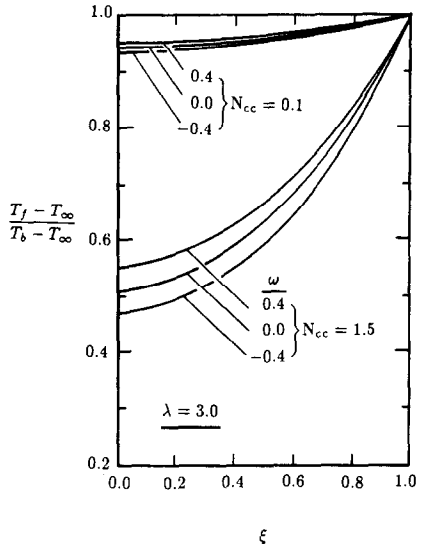

FIG. 2. Fin temperature distribution for $\lambda = 3.0$.

The local heat transfer coefficient is defined as

$$h(x) = \frac{-k\left.\frac{\partial T}{\partial r}\right|_{r=r_0}}{T_f - T_\infty} \tag{49}$$

which may be cast in dimensionless form as

$$\frac{hL}{k\sqrt{Ra}} = -\frac{1}{2}\frac{\theta'(\xi, 0)}{\sqrt{\xi}\theta_f(\xi)}. \tag{50}$$

Representative distributions of this quantity vs ξ for $\lambda = 1.0$ and 3.0, and selected values of N_{cc} and ω are presented in Figs. 3 and 4. It is observed that for small values of N_{cc} ($N_{cc} = 0.1$) the local heat transfer coefficients behave like those for isothermal boundary conditions. The coefficients decrease along the increasing streamwise direction. For larger values of N_{cc} ($N_{cc} = 1.5$), the coefficients decrease at first, reach a minimum value, and then increase with increasing streamwise direction. This is due to an enhanced buoyancy force encountered as the fluid passes from the fin tip to fin base. For a fixed value of N_{cc}, it is seen that withdrawal of fluid gives rise to higher local heat transfer coefficients. Also, for given values of N_{cc} and ω, higher local heat transfer coefficients are seen at larger values of λ.

The average heat transfer coefficient can be obtained by integrating the local heat transfer coefficient over the fin surface, and then dividing by the length of the fin, i.e.

$$\bar{h} = \frac{1}{L}\int_0^L h(x)\,dx \tag{51}$$

or in dimensionless form

$$\frac{\bar{h}L}{k\sqrt{Ra}} = \int_0^1 h^*(\xi)\,d\xi. \tag{52}$$

The numerical results of this quantity are plotted in

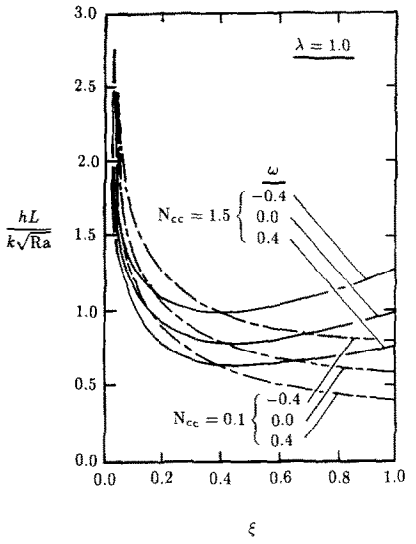

FIG. 3. Local heat transfer coefficient for $\lambda = 1.0$.

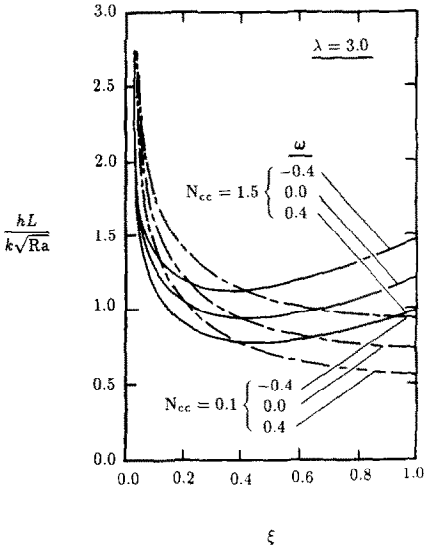

FIG. 4. Local heat transfer coefficient for $\lambda = 3.0$.

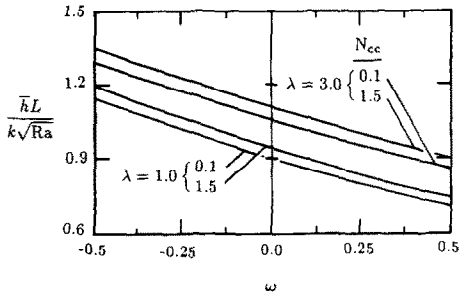

FIG. 5. Average heat transfer coefficient.

Fig. 5. It is clear that as a consequence of higher local heat transfer coefficients for smaller values of ω, higher values of average heat transfer coefficients prevail for smaller ω. Also we note an increase of average heat transfer coefficients with increasing λ or N_{cc}.

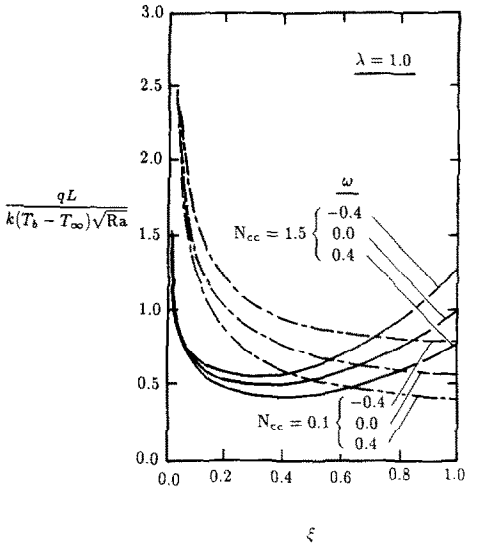

FIG. 6. Local heat flux for $\lambda = 1.0$.

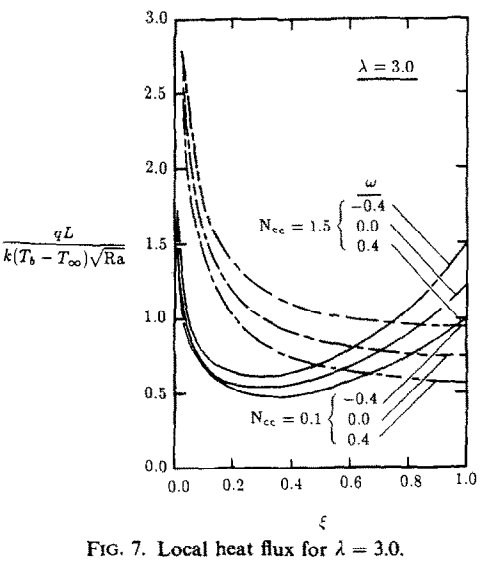

FIG. 7. Local heat flux for $\lambda = 3.0$.

The local heat flux can be expressed as

$$q = -k\frac{\partial T}{\partial r}\bigg|_{r=r_0} \tag{53}$$

which can be cast in dimensionless form as

$$\frac{qL}{k(T_b - T_\infty)\sqrt{Ra}} = -\frac{\theta'(\xi,0)}{2\sqrt{\xi}}. \tag{54}$$

The results of dimensionless local heat fluxes are given in Figs. 6 and 7. It can be seen that for a given value of λ, a decrease of ω increases the local heat fluxes.

Comparing Fig. 6 with Fig. 7, one can see that the local heat fluxes for larger values of λ are higher than those for small λ. However, one should note that the radius of a fin could be different for each λ. Thus, lower values of local heat fluxes for smaller λ's do not necessarily imply that total heat transfer rates over the fin surface are lower than those for larger λ's. This will be discussed further below.

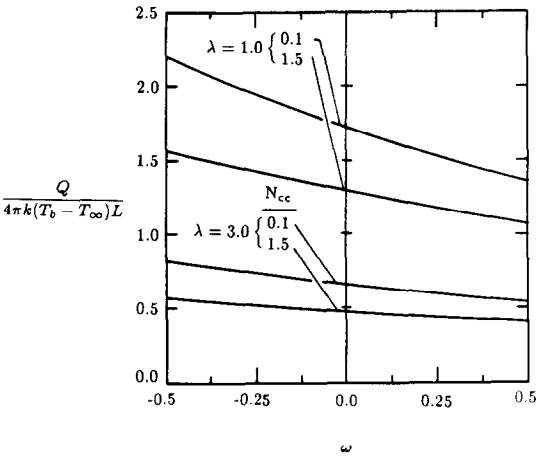

FIG. 8. Total heat transfer rate.

The total heat transfer rate over the fin surface can be obtained from

$$Q = 2\pi r_0 \int_0^L q(x)\,dx$$

$$= 2\pi r_0 \int_0^L -k\frac{\partial T}{\partial r}\bigg|_{r=r_0} dx \qquad (55)$$

which can be rewritten as

$$\frac{Q}{4\pi k(T_b - T_\infty)L} = \frac{2}{\lambda}\int_0^1 h^*(\xi)\theta_f(\xi)\,d\xi. \qquad (56)$$

Numerical results of the quantity on the left-hand side of equation (56) vs ω are plotted in Fig. 8 for representative values of N_{cc} and λ. It can be seen that the total heat transfer rates decrease as ω increases. This is in agreement with the previous results for local heat fluxes. It also shows that for fixed values of λ, an increase of N_{cc} results in a decrease of total heat transfer rate. Also it is seen that smaller values of λ give rise to higher values of the total heat transfer rate. This was expected, since a smaller value of λ represents a larger value of r_0 (i.e. larger convection surfaces), and therefore results in a larger value of the total heat transfer rate.

CONCLUDING REMARKS

The present analysis has yielded the solution of the problem of conjugate natural convection from a vertical cylindrical fin embedded in a porous medium and with a uniform lateral mass transfer specified at the surface. It was shown that higher values of conjugate convection conduction parameter N_{cc} result in nonmonotonical local heat transfer distributions. The effect of withdrawal of fluid is to increase the fin temperature variation, the local heat transfer coefficient, the average heat transfer coefficient, the local heat flux and the total heat transfer rate, and injection results in reverse effects.

REFERENCES

1. E. M. Sparrow and S. Acharya, A natural convection fin with a solution-determined nonmonotonically varying heat transfer coefficient, *J. Heat Transfer* **103**, 218–225 (1981).
2. E. M. Sparrow and M. K. Chyu, Conjugated forced convection–conduction analysis of heat transfer in a plate fin, *J. Heat Transfer* **104**, 204–206 (1982).
3. M.-J. Huang and C.-K. Chen, Vertical circular pin with conjugated forced convection–conduction flow, *J. Heat Transfer* **106**, 658–661 (1984).
4. M.-J. Huang and C.-K. Chen, Conjugated mixed convection and conduction heat transfer along a vertical circular pin, *Int. J. Heat Mass Transfer* **28**, 523–529 (1985).
5. B. Sunden, Conjugate mixed convection heat transfer from a vertical rectangular fin, *Int. Commun. Heat Mass Transfer* **10**, 267–276 (1983).
6. Jin-Yuan Liu, W. J. Minkowycz and P. Cheng, Conjugate mixed convection heat transfer analysis for a plate fin embedded in a porous medium, *Num. Heat Transfer* **9**, 575–590 (1986).
7. Jin-Yuan Liu, W. J. Minkowycz and P. Cheng, Conjugate mixed convection–conduction heat transfer along a cylindrical fin in a porous medium, *Int. J. Heat Mass Transfer* **29**, 769–775 (1986).
8. W. J. Minkowycz and P. Cheng, Free convection about a vertical cylinder embedded in a porous medium, *Int. J. Heat Mass Transfer* **19**, 805–813 (1976).
9. A. Yücel, The influence of injection or withdrawal of fluid on free convection about a vertical cylinder in a porous medium, *Num. Heat Transfer* **7**, 483–493 (1984).
10. W. J. Minkowycz and E. M. Sparrow, Numerical solution scheme for local nonsimilarity boundary-layer analysis, *Num. Heat Transfer* **1**, 69–85 (1978).
11. W. J. Minkowycz and E. M. Sparrow, Interaction between surface mass transfer and transverse curvature in natural convection boundary layers, *Int. J. Heat Mass Transfer* **22**, 1445–1454 (1979).

CONVECTION NATURELLE CONJUGUEE AUTOUR D'UNE AILETTE CYLINDRIQUE VERTICALE AVEC FLUX MASSIQUE LATERAL, DANS UN MILIEU POREUX SATURE

Résumé—On étudie numériquement le problème de la convection naturelle conjuguée autour d'une ailette cylindrique verticale avec un flux massique latéral uniforme, dans un milieu poreux saturé de fluide. Des solutions basées sur le troisième niveau de troncature sont obtenues par une méthode non similaire locale. Les effets du flux massique à la surface sont présentés ainsi que ceux du paramètre de conjugaison convection–conduction et ceux de la courbure de la surface sur la distribution de la température dans l'ailette et sur les coefficients locaux et globaux de transfert de chaleur. Une comparaison avec des solutions aux différences finies pour le cas de température pariétale constante montre un bon accord.

KOMBINIERTE NATÜRLICHE KONVEKTION AN EINER SENKRECHTEN, ZYLINDRISCHEN RIPPE BEI QUERSTRÖMUNG IN EINEM GESÄTTIGTEN PORÖSEN MEDIUM

Zusammenfassung—Der Fall der kombinierten natürlichen Konvektion an einer senkrechten, zylindrischen Rippe bei einheitlicher Querströmung in einem fluid-gesättigten porösen Medium wurde numerisch untersucht. Mit Hilfe der Methode der lokalen Unähnlichkeit wurden Lösungen durch Abbruch nach dem dritten Term ermittelt. Der Einfluß von Massenstrom, kombiniertem Konvektions–Leitungs-Parameter und Oberflächenkrümmung auf die Rippentemperaturverteilung, den örtlichen und mittleren Wärmeübergangskoeffizienten, die örtliche Wärmestromdichte und die gesamte Wärmeleistung werden dargestellt. Ein Vergleich mit den Ergebnissen des Differenzenverfahrens für den Fall konstanter Oberflächentemperatur wurde durchgeführt und ergab gute Übereinstimmung.

СОПРЯЖЕННАЯ ЗАДАЧА ЕСТЕСТВЕННОЙ КОНВЕКЦИИ У ВЕРТИКАЛЬНОГО ЦИЛИНДРИЧЕСКОГО РЕБРА С ПОПЕРЕЧНЫМ ПОТОКОМ МАССЫ В НАСЫЩЕННУЮ ПОРИСТУЮ СРЕДУ

Аннотация—Численно исследуется задача сопряженной естественной конвекции около вертикального цилиндрического ребра с однородным поперечным потоком массы в насыщенную жидкостью пористую среду. Решения с точностью до членов третьего порядка малости получены методом локальной неавтомодельности. Найдено влияние поверхностного потока массы, параметра сопряжения и кривизны поверхности на распределение температуры в ребре, местный коэффициент теплоотдачи, местную плотность теплового потока, средний коэффициент теплоотдачи и общий тепловой поток. Полученные результаты хорошо согласуются с решениями, полученными методом конечных разностей для случая постоянной температуры стенки.